Deformations and electromagnetic moments in carbon and neon isotopes

H. Sagawa,* X. R. Zhou,† and X. Z. Zhang‡
Center for Mathematical Sciences, University of Aizu, Aizu-Wakamatsu, Fukushima 965-8560, Japan

Toshio Suzuki
Department of Physics, College of Humanities and Sciences, Nihon University, Sakurajosui 3-25-40, Setagaya-ku, Tokyo 156-8550, Japan

(Received 2 July 2004; published 18 November 2004)

Static and dynamic quadrupole moments of C and Ne isotopes are investigated by using the deformed Skyrme Hartree-Fock model and also shell model wave functions with isospin-dependent core polarization charges. We point out that the deformations of C and Ne isotopes have a strong isotope dependence as a manifestation of spontaneous symmetry breaking effect in nuclear physics. The effect of spontaneous symmetry breaking is a general phenomenon known in many fields of physics. It is shown at the same time that the quadrupole moments Q and the magnetic moments μ of the odd C and odd Ne isotopes depend clearly on assigned configurations, and their experimental data will be useful to determine the deformations of the ground states of nuclei near the neutron drip line. Electric quadrupole ($E2$) transitions in even C and Ne isotopes are also studied using the polarization charges obtained by the particle vibration coupling model with shell model wave functions. Although the observed isotope dependence of the $E2$ transition strength is reproduced properly in both C and Ne isotopes, the calculated strength overestimates an extremely small observed value in ^{16}C.

DOI: 10.1103/PhysRevC.70.054316 PACS number(s): 21.10.Ky, 21.60.Cs, 21.60.Jz, 23.20.−g

I. INTRODUCTION

Nuclei far from the stability lines open a new test ground for nuclear models. Recently, many experimental and theoretical efforts have been paid to study structure and reaction mechanism in nuclei near drip lines. Modern radioactive nuclear beams and experimental detectors reveal several unexpected structure of light nuclei with the mass number $A \sim 10-24$ such as the existence of halo and skins [1], modifications of shell closures [2], and Pigmy resonances in electric dipole transitions [3]. One of the current topics is a large quenching of the electric quadrupole ($E2$) transition between the first excited 2^+ state and the ground state in ^{16}C [4,5]. The physical mechanism of these phenomena might originated from a large asymmetry of mean fields between protons and neutrons as well as the large extension of the wave functions.

Electromagnetic observables will provide useful information to study the structure of nuclei, not only ground states but also excited states. Namely, these observables are expected to pin down precise information of deformations and unknown spin parities of both stable and unstable nuclei since the deformation is intimately related to observables such as Q moments and $E2$ transitions. The magnetic moments will also give empirical information of deformation in comparison with the single-particle value (Schmidt value) in the spherical limit. The isotope dependence of the deformation is an interesting subject to study in relation to a manifestation of the spontaneous symmetry breaking effect from the beginning of one closed shell to the next closed shell. To this end, carbon and neon might be promising in future experiments within the next few years. The effect of spontaneous symmetry breaking effect is a general phenomenon known in many fields of physics. In molecular physics, spontaneous symmetry breaking was discovered by Jahn and Teller in 1937 [6]. There is a very similar fundamental mechanism in nuclear physics and molecular physics, which is responsible for causing deformations in the ground state. The coupling to the quadrupole vibration is the main origin of the static deformation in atomic nuclei [7]. On the other hand, the pairing correlations in nuclei work to stabilize the spherical symmetry. A unique and essential feature of the Jahn-Teller effect in atomic nuclei will manifest itself in the competiton between the deformations derived from particle-vibration coupling and the pairing correlations [8].

Until now, the isotope dependence of the deformation has been discussed mainly in rare earth nuclei. However, it is rather difficult in heavy nuclei to study the deformation changes systematically between two closed shells. Thus theoretical and experimental studies of the isotope dependence of deformations in light nuclei is quite an interesting subject in the context of the nuclear Jahn-Teller effect. Thus, we perform deformed Skyrme Hartree-Fock (HF) calculations with density-dependent pairing interactions in light nuclei with $A \sim 10-30$. We will study deformations of C and Ne isotopes as typical light open shell nuclei. Calculated Q moments and magnetic moments are compared with empirical data to establish the isotope dependence of deformations in these nuclei.

In light and medium mass nuclei, the shell model has been known as one of the most successful models in describing the nuclear structure in both the ground state and the excited state [9]. From a theoretical point of view, it is inter-

*Electronic address: sagawa@u-aizu.ac.jp
†On leave from Department of Physics, Tsinghua University, Beijing, China.
‡On leave from China Institute of Atomic Energy, Beijing, China.

esting to see how many differences and similarities will appear between the results of standard shell model calculations and those of the mean field theories. Thus we perform shell model calculations of electromagnetic moments in order to compare with those of deformed HF calculations.

The effective charges have been used commonly in the shell model calculations to study Q moments and $E2$ transitions. The microscopic origin has been traced back to the coupling between single-particle states and collective giant resonances [10]. This physical mechanism gives rise to the core polarization charges, which are predicted to have a strong isospin dependence in light nuclei [11,12]. Namely, the core polarization charges are larger in proton-rich nuclei and smaller in neutron-rich nuclei. A strong isospin dependence of the core polarization charges is confirmed experimentally in the study of Q moments of B isotopes [13]. In this paper, shell model calculations are performed with two effective interactions: Millener-Kurath (MK) [14] and Warburton-Brown (WBP) [15] interactions. Then, we apply the isospin-dependent core polarization charges with HF wave functions to study Q moments of odd C and Ne isotopes and $E2$ transitions in even C and Ne isotopes. These results are compared with those obtained by a standard shell model calculation with harmonic oscillator (HO) wave functions and constant effective charges. For C isotopes, Q moments and magnetic moments mainly for the ground states as well as the electric dipole transition strength were studied [16] by shell model calculations with the use of the WBP interaction. Here, we extend our investigation to both C and Ne isotopes including excited states also, and compare with the deformed HF calculations. The effects of $\delta g_\ell^{\mathrm{IV}}$ in the magnetic momemts due to the meson-exchange currents are also investigated.

This paper is organized as follows. The deformed HF calculations of C and Ne isotopes with Skyrme and density-dependent pairing interactions are presented in Sec. II. The HF wave functions are applied to predict the spin parity of C isotopes far from the stability line with study of the Q moments and the magnetic moments μ in Sec. III. The electromagnetic moments are also studied by using the shell model wave functions with the isospin-dependent effective charges and compared with the results with deformed HF wave functions in Sec. III. The $E2$ transitions are calculated by using shell model wave functions with effective charges in Sec. IV. We adopt two different models with shell model wave functions in the calculations of Q moments and $E2$ transitions. The first one is commonly used constant effective charge with the HO wave functions. The second one is a model with HF wave functions with core polarization charges obtained by the particle-vibration (PV) coupling model. A summary is given in Sec. V.

II. DEFORMED HF CALCULATIONS WITH SKYRME INTERACTIONS

We investigate the neutron number dependence of deformation properties along the chain of C and Ne isotopes. To this end, we perform deformed HF+BCS calculations with two Skyrme interactions SGII and SIII to see the interaction

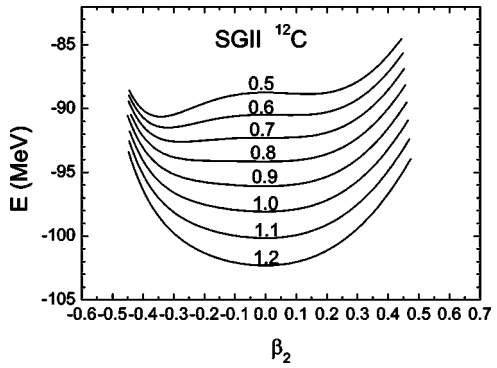

FIG. 1. Deformed HF+BCS calculations for ^{12}C with the SGII interaction. The density-dependent pairing interaction (1) is adopted in the calculations. The strength of spin-orbit force is modified multiplying a factor (0.5–1.2) by the original one in the HF calculations in C isotopes. See text for details.

dependence of the results. Both interactions are commonly used in mean field calculations and also random phase approximations for the excited states. Essential differences of the two interactions are nuclear incompressibility and spin properties. We expect some differences in the results of the two interactions in the magnitude and sign of deformations, especially, in odd nuclei. However, we found that the two interactions give essentially the same results as far as the deformations are concerned. Therefore we will mainly discuss the results of the SGII interaction hereafter. The axial symmetry is assumed for the HF deformed potential. The pairing interaction is taken to be a density-dependent pairing interaction in the BCS approximation:

$$V(\mathbf{r}_1,\mathbf{r}_2) = V_0'\left(1-\frac{\rho(r)}{\rho_0}\right)\delta(\mathbf{r}_1-\mathbf{r}_2), \tag{1}$$

where $\rho(r)$ is the HF density at $\mathbf{r}=(\mathbf{r}_1+\mathbf{r}_2)/2$ and ρ_0 is chosen to be 0.16 fm^{-3}. The pairing strength is taken to be V_0' $=-410$ MeV fm^3 for both neutrons and protons [17]. A smooth energy cutoff is employed in the BCS calculations [18].

In Fig. 1, the energy surfaces of ^{12}C are shown multiplying a factor (0.5–1.2) by the original spin-orbit interaction. Since an interplay between the single-particle energy difference around the Fermi surface and the quadrupole vibration energy plays an essential role for driving the deformation, the smaller spin-orbit splitting gives a clear deformation minimum on the oblate side. The original spin-orbit interactions of SGII and SIII give the energy minima at a spherical shape for ^{12}C. In the case of Ne isotopes, the original spin-orbit interaction works to predict well the isotope dependence of the deformation in comparison with emirical data. This is due to the fact that the $1d_{5/2}$ and $2s_{1/2}$ states are rather close in energy in the spherical HF results in Ne isotopes, while $1p_{1/2}$ and $1p_{3/2}$ states are not close enough to drive the deformation in ^{12}C for the HF results of C isotopes. In order to make a realistic deforamation minima in C isotopes, we reduce the spin-orbit interaction of SGII to be 60% of the original strength, while the original one is used in Ne isotopes. Since our main aim of this study is the isotope depen-

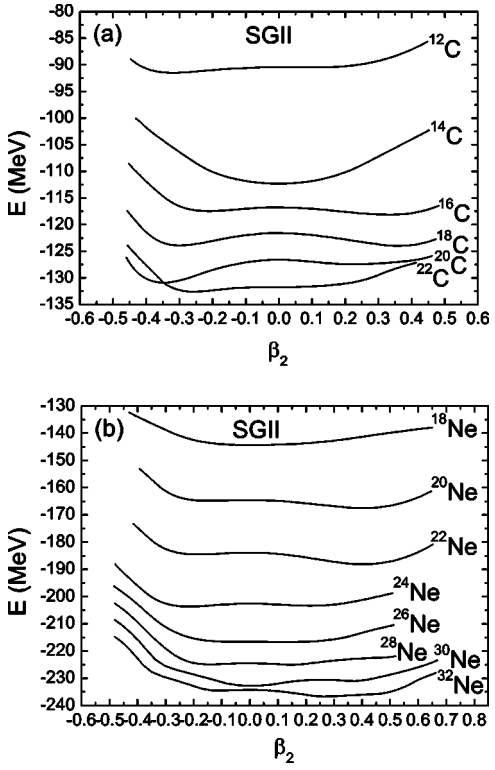

FIG. 2. Deformed HF+BCS calculations with the SGII interaction (a) for C isotopes and (b) for Ne isotopes. The density-dependent pairing interaction (1) is adopted in the calculations. The strength of spin-orbit force is modified to be 60% of the original one in the HF calculations in C isotopes. See the text for details.

dence of the deformation, the HF results should give a proper deformation in a known case like ^{12}C, while the smaller spin-orbit interaction may give poorer results than the original one for the total binding energies. This is the reason why we adopt the smaller spin-orbit force in C isotopes.

Figure 2 shows the binding energy surfaces for even-mass C and Ne isotopes as a function of the quadrupole deformation parameter β_2 with SGII interaction. The deformations at the energy minima are tabulated in Table I for C isotopes and Table II for Ne isotopes with SGII interaction.

The energy minimum in ^{12}C appears at an oblate deformation with $\beta_2=-0.32$ in Fig. 2(a). The energy minimum becomes spherical in ^{14}C because of the neutron closed shell effect. For heavier C isotopes, ^{16}C shows a large prolate minimum, while in ^{18}C, two minima appear both in the prolate and oblate sides having almost the same energies. Namely, the ground state has a minimum with a large prolate deformation at $\beta_2=0.36$, while a local minimum appears at the oblate side at $\beta_2\sim-0.3$ within an energy difference of 0.1 MeV. The deformation becomes oblate in ^{20}C and ^{22}C. The HF calculations with the original spin-orbit strength gives a spherical shape for ^{12}C and ^{22}C.

The deformation of Ne isotopes are shown in Fig. 2(b) and Table II. In general, the energy surface is shallow in even Ne isotopes. The energy minimum of ^{18}Ne is very close to spherical shape as is expected due to $N=8$ shell closure. The prolate deformations are found in ^{20}Ne and ^{22}Ne and then the deformation minimum is oblate in ^{24}Ne. The spherical and oblate energy minima are almost degenerate in energy in ^{26}Ne. The energy minimum of ^{28}Ne is very flat and depends on the adopted interaction. Namely the SGII interaction gives a prolate minimum, while the SIII interaction gives an oblate minimum. The nucleus ^{30}Ne is found to show a spherical shape due to another shell closure at $N=20$. Then, ^{32}Ne becomes prolate again as a typical nucleus next to the closed shell nucleus.

A deformed Skyrme HF+ blocked BCS calculation are performed for odd C and Ne isotopes and the results are shown in Fig. 3 for C isotopes and Fig. 4 for Ne isotope. The deformation and the intrinsic Q_0 moments are tabulated in Table I for C isotopes and in Table II for Ne isotopes with the SGII interaction. In ^{15}C, having one extra neutron outside of the neutron closed shell $N=8$, the spin parity of the ground state is given to be $J^\pi=1/2^+$ with a prolate deformation by the deformed HF calculation, while a simple shell model configuration is $J^\pi=5/2^+$ and the Q moment has a negative value (an oblate shape in the intrinsic moment). The experimental assignment of the spin parity is $J^\pi=1/2^+$ in the ground state of ^{15}C. This is also a typical example of the deformation effect in the nuclear system.

The results shows that the ground state of ^{17}C is prolate with $J^\pi=\frac{3}{2}^+$ while that of ^{19}C is oblate with $J^\pi=\frac{3}{2}^+$. In ^{19}C, the energy minimum of $J^\pi=\frac{1}{2}^+$ is almost degenerate with that of $J^\pi=\frac{3}{2}^+$ with almost the same oblate deformation $\beta_2\sim-0.36$. These spin parities of the ground states are consistent with the shell model calculations [17]. The spin of the ground state of ^{17}C has been assigned as $3/2^+$ in the magnetic moment measurement [19] as will be discussed later. The spin of ^{19}C is assigned as $1/2^+$ in the Coulomb breakup reactions [20], while there is still controversy about the experimental assignment in Ref. [21]. The HF results of odd Ne isotopes are shown in Fig. 4. In ^{19}Ne, with one neutron outside of the $N=8$ neutron core, one can see again a prolate deformation in the ground state with $J^\pi=\frac{1}{2}^+$ as a clear sign of the isotope dependence of the deformation expected from the nuclear Jahn-Teller effect. The prolate deformation becomes larger in ^{21}Ne having three neutrons outside of the $N=8$ neutron core than that of ^{19}Ne. The spin parities of the ground states in $^{19-23}$Ne agree with the experimental data, while the spin parity of the ground state in ^{25}Ne is not yet determined experimentally.

The isotope dependence of the energy minima is shown in Fig. 5 as a function of neutron number N. The oblate deformation is obtained in ^{12}C as is expected from the two hole configurations to the closed shell $N=Z=8$. The shape becomes spherical in $N=8$ isotones ^{14}C and ^{18}Ne due to the neutron closed shell effect. Then two isotopes show large prolate deformations in nuclei with $11\geqslant N>8$. While a naive shell model gives $J^\pi=\frac{5}{2}^+$ with negative Q moments for $N=9$ isotones ^{15}C and ^{19}Ne, the deformed HF gives the prolate shape, i.e., positive intrinsic Q_0 moments and also positive Q moments at the band head with $J^\pi=1/2$. There is a sharp change of the deformation minima from prolate to oblate between $N=12$ and 14 for both C and Ne isotopes. The shape becomes close to spherical in very heavier Ne isotopes near $N=20$. In this way, the two isotopes show a clear manifestation of the the nuclear deformation effect in the de-

TABLE I. Energies, deformations, and intrinsic Q_0 moments in Eqs. (4) and (5) in carbon isotopes with the Skyrme interaction SGII. The intrinsic g_K factor in Eq. (10), the decoupling parameter b in Eq. (12), and the magnetic moments μ in Eqs. (8) and (11) are also listed. The spin-orbit interaction is multiplied by a factor 0.6 to induce clear deformation minima in C isotopes.

Nucleus	K^π	Energy (MeV)	β_{2p}	β_{2n}	β_2	Q_{0p} (fm^2)	Q_{0n} (fm^2)	g_k	b	μ
^{9}C	$1/2^-$	0.0	0.273	0.251	0.269	16.260	10.148	−3.619	1.039	1.103
	$3/2^-$	0.98	−0.293	−0.196	−0.279	−17.181	−5.743	−1.273	0.0	−0.746
^{10}C	0^+	0.0	−0.277	−0.283	−0.279	−13.830	−7.923			
	0^+	0.04	0.285	0.476	0.355	14.839	14.262			
^{11}C	$1/2^-$	0.0	−0.360	−0.358	−0.359	−18.777	−14.233	3.375	−0.117	0.855
	$3/2^-$	0.58	0.210	0.395	0.277	8.913	7.521	−1.273	0.0	−0.818
	$3/2^-$	1.09	−0.332	−0.318	−0.327	−17.170	−13.311	−1.273	0.0	−0.818
^{12}C	0^+	0.0	−0.319	−0.317	−0.318	−15.630	−15.316			
	0^+	0.99	0.090	0.089	0.090	4.107	4.019			
^{13}C	$1/2^-$	0.0	0.058	0.057	0.057	2.630	1.919	1.973	−0.589	0.779
	$5/2^+$	5.97	−0.420	−0.419	−0.420	−22.492	−30.642	−0.764	0.0	−1.035
	$1/2^+$	6.15	0.378	0.376	0.377	19.001	35.287	−3.456	1.070	0.975
	$1/2^+$	6.95	−0.405	−0.404	−0.405	−21.399	−27.791	−3.518	1.033	0.938
^{14}C	0^+	0.0	0.013	0.005	0.008	0.591	0.333			
^{15}C	$1/2^+$	0.0	0.247	0.166	0.199	11.938	27.246	−3.221	−1.107	−1.739
	$5/2^+$	1.35	−0.217	−0.117	−0.158	−10.381	−15.732	−0.764	0.0	−1.079
	$1/2^+$	2.26	−0.153	−0.08	−0.11	−7.2	−13.580	−3.114	−1.087	−1.659
	$3/2^+$	2.38	0.079	0.043	0.058	3.684	5.997	−0.989	0.0	−0.650
^{16}C	0^+	0.0	0.279	0.371	0.341	13.822	38.805			
	0^+	0.61	−0.240	−0.207	−0.217	−11.822	−21.473			
^{17}C	$3/2^+$	0.0	0.330	0.422	0.392	16.751	50.712	−1.187	0.0	−0.856
	$1/2^+$	0.46	−0.326	−0.264	−0.285	−16.708	−36.162	−3.425	−1.046	−1.770
	$1/2^+$	0.75	0.303	0.258	0.273	15.415	43.283	−3.340	−1.085	−1.775
	$3/2^+$	1.19	−0.327	−0.267	−0.287	−16.674	−35.161	0.841	0.0	0.969
	$5/2^+$	1.23	−0.316	−0.262	−0.279	−16.209	−36.810	−0.764	0.0	−1.112
	$5/2^+$	2.3	0.161	0.233	0.210	7.802	16.942	−0.764	0.0	−1.112
^{18}C	0^+	0.0	0.315	0.372	0.356	16.203	51.637			
	0^+	0.1	−0.316	−0.286	−0.294	−16.444	−40.669			
^{19}C	$3/2^+$	0.0	−0.385	−0.353	−0.362	−21.012	−59.909	0.980	0.0	1.071
	$1/2^+$	0.35	−0.387	−0.337	−0.351	−21.255	−57.435	−3.493	−1.038	−1.795
	$5/2^+$	1.56	−0.376	−0.337	−0.348	−20.484	−59.018	−0.764	0.0	−1.138
	$1/2^+$	2.05	0.353	0.409	0.394	18.482	65.388	2.630	0.235	0.362
	$5/2^+$	2.28	0.243	0.310	0.292	12.211	35.644	−0.764	0.0	−1.138
	$1/2^+$	3.17	−0.229	−0.219	−0.222	−11.501	−22.367	0.106	−10.282	−0.597
	$3/2^+$	3.56	0.222	0.203	0.208	11.211	34.580	−1.116	0.0	−0.815
^{20}C	0^+	0.0	−0.371	−0.342	−0.349	−20.373	−61.980			
	0^+	3.45	0.250	0.238	0.241	12.980	42.915			
^{22}C	0^+	0.0	−0.330	−0.241	−0.258	−18.265	−54.249			
	0^+	0.84	0.060	0.031	0.037	3.088	6.679			

formed HF calculations as a spontaneous spherical symmetry breaking of the spherical shape induced by the driving force in the mean field potential [8]. The deformation effect in the C and Ne isotopes is unique compared with that in rare-earth nuclei in the sense that both prolate and oblate deformations appear clearly in the beginning of the closed shell and at the end of the closed shell. The isotope dependence of deformation in C isotopes was studied by using the antisymmetrized molecular dynamics (AMD) model in Ref. [22]. The AMD model predicts an isotope dependence of neutron deformations very similar to the present results, while the proton shapes stay always at the oblate side in the AMD model. It should be noticed that the triaxiality is discarded in the present deformed HF model. However, the present model has

TABLE II. Energies, deformations, and intrinsic Q moments in Eqs. (4) and (5) in neon isotopes with the Skyrme interaction SGII. The intrinsic g_K factor in Eq. (10), the decoupling parameter b in Eq. (12), and the magnetic moments μ in Eqs. (8) and (11) are also listed. The original spin-orbit interaction is used.

Nucleus	K^π	Energy (MeV)	β_{2p}	β_{2n}	β_2	Q_{0p} (fm^2)	Q_{0n} (fm^2)	g_k	b	μ
^{18}Ne	0^+	0.0	−0.011	−0.007	−0.009	−1.084	−0.479			
^{19}Ne	$1/2^+$	0.0	0.403	0.238	0.336	42.712	32.888	−3.063	−1.141	−1.700
	$5/2^+$	1.74	−0.167	−0.1	−0.14	−16.845	−13.844	−0.764	0.0	−0.988
	$3/2^+$	2.67	0.06	0.029	0.047	5.944	3.971	−0.870	0.0	−0.467
^{20}Ne	0^+	0.0	0.405	0.403	0.404	42.512	41.350			
	0^+	2.70	−0.157	−0.156	−0.157	−15.692	−15.206			
^{21}Ne	$3/2^+$	0.0	0.432	0.428	0.430	45.876	50.126	−1.140	0.0	−0.741
	$1/2^+$	1.84	0.377	0.273	0.325	39.399	42.450	−2.923	−1.168	−1.652
	$5/2^+$	3.29	0.334	0.332	0.333	34.162	27.898	−0.764	0.0	−1.024
	$3/2^+$	3.68	−0.169	−0.180	−0.174	−16.823	−18.527	−0.405	0.0	−0.079
	$1/2^+$	3.76	−0.222	−0.225	−0.223	−22.419	−27.835	−2.355	−1.234	−1.398
	$5/2^+$	3.99	−0.144	−0.102	−0.123	−14.318	−16.742	−0.764	0.0	−1.024
^{22}Ne	0^+	0.0	0.410	0.403	0.406	43.098	53.259			
	0^+	3.61	−0.183	−0.185	−0.184	−18.378	−23.482			
^{23}Ne	$5/2^+$	0.0	0.344	0.340	0.342	35.311	38.561	−0.764	0.0	−1.053
	$1/2^+$	1.66	−0.227	−0.222	−0.224	−23.041	−34.039	−2.393	−1.230	−1.414
	$3/2^+$	2.0	−0.220	−0.236	−0.229	−22.282	−32.548	−0.193	0.0	0.088
	$3/2^+$	2.67	0.223	0.146	0.180	22.497	21.959	−1.018	0.0	−0.655
	$5/2^+$	3.19	−0.160	−0.129	−0.143	−16.012	−23.350	−0.764	0.0	−1.054
^{24}Ne	0^+	0.0	−0.212	−0.214	−0.213	−21.511	−33.62			
	0^+	0.32	0.267	0.194	0.223	27.23	30.27			
^{25}Ne	$5/2^+$	0.0	0.314	0.286	0.297	32.823	42.450	−0.764	0.0	−1.078
	$1/2^+$	1.38	−0.104	−0.082	−0.091	−10.568	−12.990	−1.001	−1.97	−0.954
	$3/2^+$	1.62	−0.055	−0.042	−0.047	−5.579	−5.995	−0.708	0.0	−0.398
^{26}Ne	0^+	0.0	0.178	0.113	0.135	18.232	21.741			
	0^+	0.03	0.001	−0.001	−0.001	0.111	−0.253			
^{28}Ne	0^+	0.0	0.201	0.121	0.146	21.357	28.565			
	0^+	0.1	−0.158	−0.132	−0.140	−16.706	−31.012			

a reasonable predicting power for such observables as Q moments and magnetic moments, which will be discussed in Sec. III.

III. Q MOMENTS AND MAGNETIC MOMENTS IN C AND Ne ISOTOPES

A. Q moments

We study in this section Q moments and magnetic moments in C and Ne isotopes using the deformed HF wave functions and the shell model calculations [15]. We first discuss the Q moments. In the shell model calculations, two effective interactions, WBP and MK interactions, are adopted within the $0\hbar\omega$ configurations in p-sd model space as they have been among those commonly and often used and well studied. The WBP Hamiltonian is designed to reproduce systematically the energies of the ground and excited states of stable p- and sd-shell nuclei. The MK Hamiltonian is also constructed for stable p- and sd-shell nuclei, especially for p-shell nuclei including states with $p^{-1}sd$ configurations within the p-sd space.

Two kinds of effective charges are compared in the calculations. The first one is the standard constant effective charges, $e^p_{eff}=1.3$ and $e^n_{eff}=0.5$, with the harmonic oscillator wave functions. This prescription has been known to explain successfully Q moments and $B(E2)$ transitions in many stable p- and sd-shell nuclei [9]. The second one is the isospin-dependent polarization charges, e_{pol} [10,11], derived from the microscopic PV coupling model based the on the HF+random phase approximation. The calculated polarization charge e_{pol}(PV) is parametrized as

$$e_{pol}(\mathrm{PV})/e = a\frac{Z}{A} + b\frac{N-Z}{A} + \left(c + d\frac{Z}{A}\frac{N-Z}{A}\right)\tau_z,$$
$$\tau_z = 1\ (-1)\ \text{for}\ \nu(\pi), \qquad (2)$$

with $a=0.82$, $b=-0.25$, $c=0.12$, and $d=-0.36$ to reproduce the calculated values of e_{pol} for ^{12}C and ^{16}C by the HF

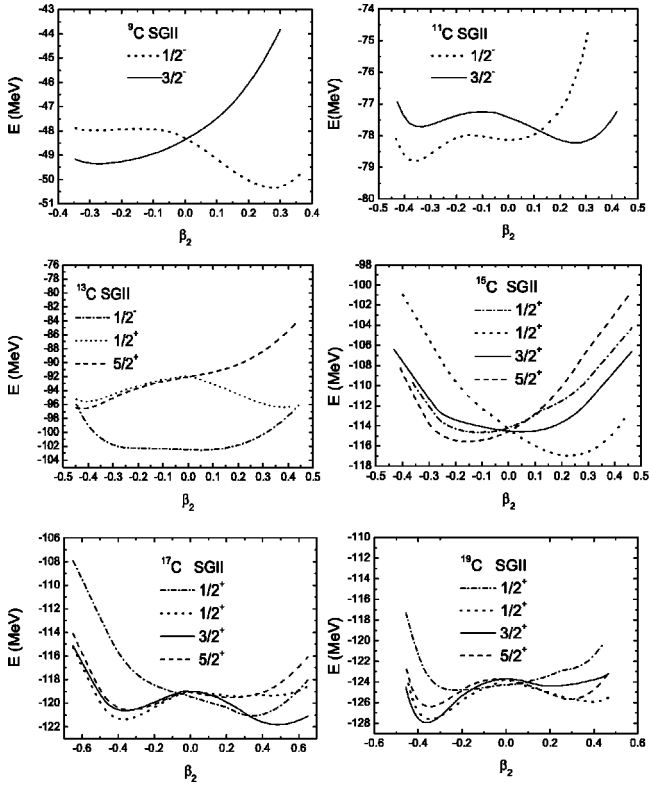

FIG. 3. Deformed HF+blocked BCS calculations with SGII interaction for odd C isotopes. See the caption to Fig. 2 and text for details.

+PV model [12]. Both the neutron (ν) and proton (π) polarization charges decrease as the neutron excess increases. The effective charges are defined by using the polarization charges (2) as

$$e^p_{eff}(\mathrm{PV})/e = 1 + e^p_{pol}(\mathrm{PV})/e,$$

$$e^n_{eff}(\mathrm{PV})/e = e^n_{pol}(\mathrm{PV})/e. \tag{3}$$

The Q moments obtained by using the polarization charges (3) are shown in Fig. 6 and Table III. In Table III, the proton and the neutron components Q_p and Q_n are also tabulated. The single particle and shell model Q moments of odd C isotopes are shown in Fig. 6(a) together with deformed HF ones. Open circles denote results of the shell model calculations with the use of $e^n_{eff}(\mathrm{PV})$. Single-particle or -hole values with the use of $e^n_{eff}(\mathrm{PV})$ are given by open triangles. Namely, the configurations for ^{9}C and ^{11}C are $\nu p_{3/2}$ and $\nu p^{-1}_{3/2}$, respectively. The single-particle configurations for ^{17}C and ^{19}C are $\nu d_{5/2}1s^2_{1/2}(J=0)$ and $\nu d^{-1}_{5/2}$, respectively, for the $5/2^+$ state. A single-particle configuration $\nu d_{3/2}$ is taken as the $3/2^+$ state of ^{17}C. Filled triangles denote the configurations of the seniority 3 states with two particles (holes) in $\nu d_{5/2}$ orbit, namely, $\nu d^{\pm 2}_{5/2}(J=2)1s_{1/2}$ configuration for $J^\pi=3/2^+$ and $5/2^+$. The $\nu d^2_{5/2}(J=2)1s_{1/2}$ and $\nu d^{-2}_{5/2}(J=2)1s_{1/2}$ are possible simple configurations for ^{17}C and ^{19}C, respectively, to give nonzero values of Q moments, since the $\nu d^3_{5/2}$ or $\nu d^3_{5/2}1s^2_{1/2}$ configuration corresponding to the middle of the $d_{5/2}$ shell results in the vanishing of the Q moments.

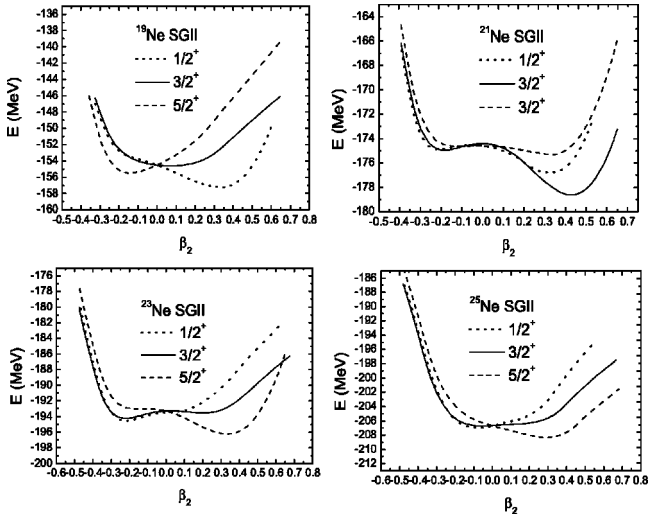

FIG. 4. Deformed HF+blocked BCS calculations with the SGII interaction for odd Ne isotopes. See the caption to Fig. 2 and text for details.

The Q moments are analytically obtained to be $\mp\frac{2}{5}e^n_{eff}Q_{sp}(d_{5/2})$ for $3/2^+$ and $\mp\frac{4}{7}e^n_{eff}Q_{sp}(d_{5/2})$ for $5/2^+$ in the case of the $\nu d^{\pm 2}_{5/2}(J=2)1s_{1/2}$ configuration. Here, $Q_{sp}(d_{5/2})$ denotes the single particle value of the Q moment for the $d_{5/2}$ orbit. Note that the signs of the Q moments for ^{17}C and ^{19}C are opposite. The shell model values of the Q moments are obtained by the admixture among these configurations, and their magnitudes are enhanced a few times larger than those of the simple configurations. Nevertheless, the difference of the signs between ^{17}C and ^{19}C can be understood from those of the simple configurations.

Let us now discuss the Q moments of C and Ne isotopes with the deformed HF calculations. In Tables I and II the deformations and the intrinsic Q_0 moments at the energy minima of deformed HF calculations are summarized both for C and Ne isotopes. The intrinsic Q_{0p} and Q_{0n} moments are calculated by using HF wave function $|K\rangle$,

$$Q_{0p} = \left\langle K \left| \int \hat{\rho}_p(x,y,z)(2z^2 - x^2 - y^2)d\mathbf{r} \right| K \right\rangle, \tag{4}$$

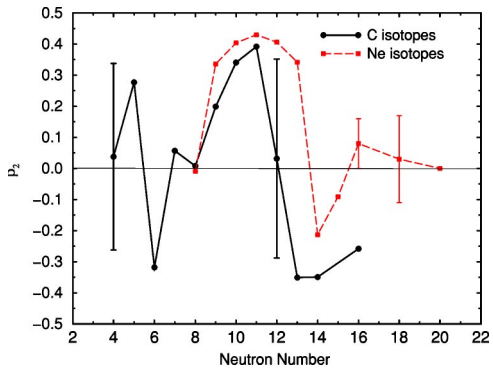

FIG. 5. (Color online) Isotope dependence of deformations of C and Ne isotopes with SGII interaction. The points with error bars show the cases in which two deformation minima are found within the energy difference of 0.1 MeV.

TABLE III. Q moments in C and Ne isotopes. The shell model calculations are performed by using the isospin-dependent effective charges (3), while the HF results are obtained by using Skyrme interactions SGII and SIII. We take $K=J$ in odd isotopes and the values $K=0$ and $J=2$ are used in ^{20}Ne and ^{22}Ne. The experimental data are taken from Ref. [24]. The data sandwiched by bars are known only in the absolute magnitudes. The numbers in parentheses show experimental uncertainties.

		WBP			MK			SGII	SIII	
Nucleus	J^π	Q_p (fm^2)	Q_n (fm^2)	Q (e fm^2)	Q_p (fm^2)	Q_n (fm^2)	Q (e fm^2)	Q (e fm^2)	Q (e fm^2)	Q (expt) (e fm^2)
^{9}C	$3/2^-$	−1.32	−2.40	−3.88	−1.94	−2.24	−4.63	−3.44	−3.40	——
^{11}C	$3/2^-$	2.76	0.983	4.27	2.90	1.47	4.76	1.79	1.94	|3.426|
^{17}C	$3/2^+$	0.57	5.84	2.39	0.94	6.10	2.89	3.35	3.27	——
^{19}C	$3/2^+$	−1.29	−6.50	−3.00	−1.51	−6.40	−3.21	−4.20	−4.00	——
^{19}C	$5/2^+$	1.37	6.67	3.13	0.083	−0.578	−0.051	−7.31	−6.65	——
^{20}Ne	2^+	−8.43	−8.43	−15.34	−8.62	−8.62	−15.69	−12.3	−11.3	−23(3)
^{21}Ne	$3/2^+$	5.62	6.75	10.43	5.83	7.02	10.82	9.18	8.64	+10.3(8)
^{22}Ne	2^+	−7.57	−9.88	−13.92	−8.25	−10.44	−15.02	−12.61	−11.33	−19(4)
^{23}Ne	$5/2^+$	8.02	10.04	14.07	−6.55	−7.96	−11.51	12.31	10.87	——
^{25}Ne	$3/2^+$	−4.86	−4.94	−7.59	−4.96	−7.47	−8.65	−1.12	−1.02	——
^{25}Ne	$5/2^+$	−3.37	1.49	−3.45	7.21	9.26	11.98	11.72	9.91	——

$$Q_{0n} = \left\langle K \left| \int \hat{\rho}_n(x,y,z)(2z^2 - x^2 - y^2) d\mathbf{r} \right| K \right\rangle, \qquad (5)$$

where $\hat{\rho}_p$ and $\hat{\rho}_n$ are the proton and the neutron density operators, respectively. The quadrupole deformations β_{2p}, β_{2n} are proton and neutron deformations at the minimum points of neutron and proton energy surfaces, while the value β_2 is obtained at the minimum point of total energy surface. The sign of deformation is always the same for protons and neutrons, while the magnitude is largely different in several configurations, for example, the β_{2p} of the ground state of ^{15}C is much larger than the β_{2n}, while the β_{2n} values are larger than those of the β_{2p} in $^{16-18}$C.

The Q moment in the laboratory system can be expressed as

$$Q = eQ_{0p}\frac{3K^2 - J(J+1)}{(2J+3)(J+1)}. \qquad (6)$$

We always consider the state with $K=J$ in Eq. (6) for the states in odd nuclei. Calculated Q moments by using the deformed HF wave functions are tabulated in Table III together with the shell model results. For C isotopes, the deformed HF results with SGII interaction are shown in Fig. 6(a) by the open boxes. In C isotopes, it is remarkable that the HF results are very close to the shell model ones in most of the cases except $5/2^+$ state in ^{19}C. Although the two results are surprisingly consistent quantitatively in several cases, the shell model wave functions with the isospin-dependent effective charges give somewhat better agreement with available experimental data in Q moments.

In Table III, we see that the Q moments of ^{19}C $(5/2^+)$, ^{23}Ne $(5/2^+)$, and ^{25}Ne $(5/2^+)$ obtained by the shell model calculations with the WBP and MK interactions have opposite signs. In these cases, the second $5/2_2^+$ states near the ground $5/2_1^+$ states in one interaction correspond to the $5/2_1^+$ states in the other interaction. Calculated Q moments of the $5/2_2^+$ states in ^{19}C, ^{23}Ne, and ^{25}Ne are $Q=-0.19$, -11.81, and 8.73 e fm^2 ($Q=3.07$, 13.63, and -6.12 e fm^2), respectively, for the WBP (MK) case. In the Q moments of ^{23}Ne and ^{25}Ne, the contribution from the sd mixing part is comparable or larger than that from the d-orbit part, and in particular for the Q moment of ^{25}Ne $(5/2_1^+)$ obtained by the WBP they have opposite signs and the net sign is determined by the sd mixing part.

The MK interaction has been modified by enhancing the spin-isospin part of the interaction and shell gap between the $0p_{1/2}$ and $0p_{3/2}$ orbits [23]. These modifications were found to be important for shell evolution and can affect the observables near the drip-line nuclei. We comment on the dependence of the calculated Q moments of the C isotopes on the shell model Hamiltonians. Using the modified MK (denoted as OFU*) Hamiltonian [23], which is to be applied within the $0\hbar\omega$ space, Q_p and Q_n are calculated and compared with the values obtained by the MK Hamiltonian. Calculated Q moments are found to be modified by 0.46 (10.9%), −0.08 (−1.8%), −0.10 (−3.3%), and −0.23 (−7.2% for the $3/2^+$ state) e fm^2 in ^{9}C $(3/2^-)$, ^{11}C $(3/2^-)$, ^{17}C $(3/2^+)$, and ^{19}C $(3/2^+, 5/2^+)$ states, respectively. The effects are rather small except for ^{9}C.

B. Magnetic moments

Magnetic moments are useful observables to find out the spin parities and the deformations of the ground state of nuclei and also those of the excited states. We study the magnetic moments of the ground and excited states of C and Ne isotopes performing the deformed HF and the shell model

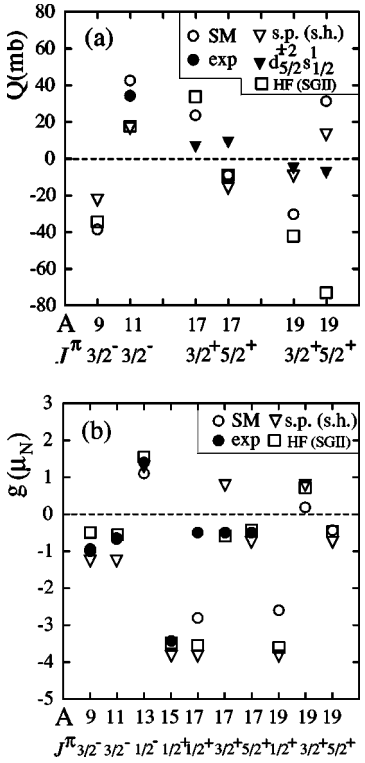

FIG. 6. Q moments and magnetic moments for the odd C isotopes. (a) Open triangles denote Q moments of single-particle or -hole values, while filled triangles give results of the $0d_{5/2}^{+2}1s_{1/2}$ configuration. These values include the effects of the polarization charges, e_{eff}(PV) in Eq. (3). (b) Open circles denote the results of the magnetic g factors of shell model calculations obtained with the use of WBP interaction and $g_s^{eff}=0.9g_s$, while the HF results are obtained by using Eqs. (8) and (11) and shown by open boxes. The filled circles are the experimental values taken from Refs. [19,25,27,30].

calculations. Slightly quenched spin g_s^{eff} factors

$$g_s^{eff} = 0.9 g_s \tag{7}$$

are used in the shell model calculations with $g_s^\nu=-3.82$ and $g_s^\pi=5.58$ in unit of the nuclear magneton $\mu_N=e\hbar/2m_pc$. The quenching factor 0.9 is somewhat different to the commonly adopted values $(0.7-0.8)g_s$. This difference might be due to smaller second-order core polarization effects in light neutron-rich nuclei [26].

For deformed HF wave functions $|K\rangle$, the magnetic moment can be written, for a band with $K>\frac{1}{2}$, as

$$\mu = g_R J + (g_K - g_R)\frac{K^2}{J+1}, \tag{8}$$

where g_R is the effective g factor for the rotational motion,

$$g_R = \frac{Z}{A}, \tag{9}$$

and g_K is the intrinsic g factor,

$$g_K = \langle K | g_l l_3 + g_s s_3 | K \rangle. \tag{10}$$

For a $K=\frac{1}{2}$ state, the magnetic moment contains an additional contribution from the $\Delta K=1$ term in the intrinsic moment,

$$\mu(K=1/2,J) = g_R J + \frac{g_K - g_R}{4(J+1)}[1 + 2(J+1)(-1)^{J+1/2} b], \tag{11}$$

where b is the magnetic decoupling parameter defined as

$$b(g_K - g_R) = \langle K=1/2 | (g_l - g_R) l_+ + (g_s - g_R) s_+ | \overline{K=1/2} \rangle. \tag{12}$$

The calculated values g_K and b are tabulated in Tables I and II.

The calculated magnetic moments of C and Ne isotopes are tabulated in Table IV together with available experimental data. Results of the shell model calculations with an effective orbital g factor in the isovector part, $\delta g_\ell^{\rm IV}=0.10$, due to the meson-exchange current contributions [28] are also shown. The inclusion of $\delta g_\ell^{\rm IV}$ improves the agreement of the calculated values with the experimental ones for the MK interaction. The root mean square (rms) deviations of the calculated magnetic moments from the experimental ones for

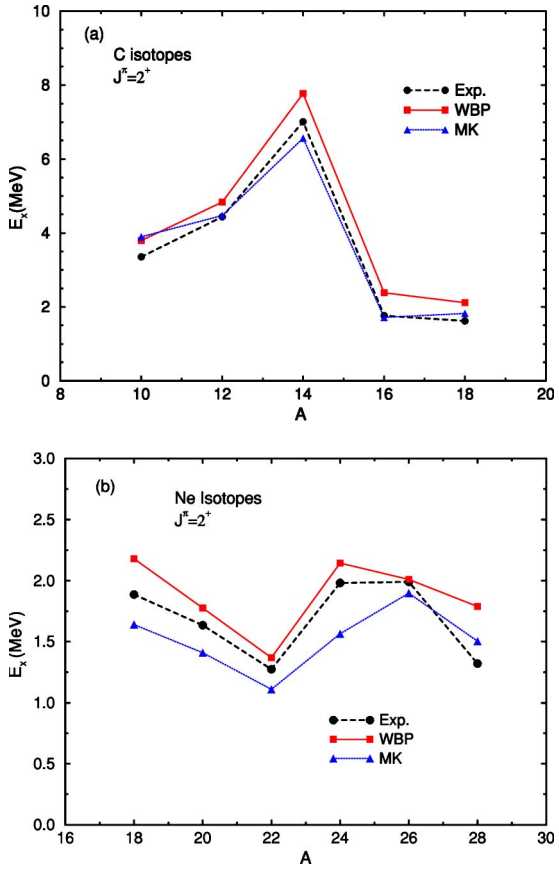

FIG. 7. (Color online) The excitation energies of the first 2^+ states: (a) C isotopes and (b) Ne isotopes. Shell model calculations are performed in $0\,\hbar\omega$ model space in the (p-sd) configurations with Warburton-Brown WBP interaction and Millener-Kurath (MK) interaction. Experimental data are taken from Ref. [29].

TABLE IV. Magnetic moments μ (in unit of nuclear magneton $e\hbar/2m_pc$) in C and Ne isotopes. The shell model calculations are performed by using the effective spin $g_s(eff)$ factor $g_s(eff)=0.9g_s(bare)$. The shell model values with the inclusion of $\delta g_\ell^{\rm IV}$ are given with in the brackets. The HF results are obtained by using Eqs. (8) and (11) with Skyrme interactions SGII and SIII. We take $K=J$ in all configurations in the table. The experimental data are taken from Ref. [25] for ^{9}C, from Ref. [24] for ^{11}C, ^{13}C, and Ne isotopes, from Ref. [27] for ^{15}C, and from Ref. [19] for ^{9}C. The data sandwiched by bars are known only in the absolute magnitudes. The numbers in parentheses show experimental uncertainties.

Nucleus	J^π	WBP($+\delta g_\ell^{\rm IV}$)	MK($+\delta g_\ell^{\rm IV}$)	SGII	SIII	Experiment
^{9}C	$3/2^-$	−1.483 (−1.553)	−1.404 (−1.472)	−0.746	−0.746	|1.3914(5)|
^{11}C	$3/2^-$	−0.991 (−1.069)	−0.691 (−0.759)	−0.818	−0.818	−0.965(2)
^{13}C	$1/2^-$	0.554 (0.482)	0.634 (0.592)	0.779	0.780	+0.7024
^{13}C	$5/2^+$	−1.277 (1.457)	−1.394 (−1.574)	−1.035	−1.035	|1.395(38)|
^{15}C	$1/2^+$	−1.721 (1.724)	−1.627 (1.631)	−1.739	−1.587	|1.720(9)|
^{15}C	$5/2^+$	−1.633 (−1.824)	−1.546 (−1.736)	−1.079	−1.079	−1.758(30)
^{17}C	$1/2^+$	−1.408 (−1.414)	−1.394 (−1.574)	−1.770	−1.743	——
^{17}C	$3/2^+$	−0.767 (−0.881)	−0.623 (−0.735)	−0.856	−0.843	|0.7581(38)|
^{17}C	$5/2^+$	−1.257 (−1.454)	−1.302 (−1.494)	−1.112	−1.112	
^{19}C	$1/2^+$	−1.305 (−1.323)	−1.374 (−1.387)	−1.795	−1.780	——
^{19}C	$3/2^+$	0.284 (0.137)	0.421 (0.273)	1.071	0.975	——
^{19}C	$5/2^+$	−1.126 (−1.319)	−0.831 (−1.024)	−1.138	−1.138	——
^{19}Ne	$1/2^+$	−1.870 (−1.911)	−1.828 (−1.865)	−1.700	−1.605	−1.88542(8)
	$5/2^+$	−0.618 (−0.639)	−0.476 (−0.475)	−0.988	−0.988	−0.740(8)
^{21}Ne	$3/2^+$	−0.718 (−0.791)	−0.775 (−0.847)	−0.741	−0.726	−0.661797(5)
	$5/2^+$	−0.522 (−0.621)	−0.527 (−0.611)	−1.024	−1.024	|0.49(35)|, |0.70(8)|
^{23}Ne	$5/2^+$	−0.996 (−1.166)	−0.360 (−0.429)	−1.053	−1.053	−1.08(1)
^{25}Ne	$1/2^+$	−0.680 (−0.712)	−0.556 (−0.605)	−0.954	−0.954	——
	$3/2^+$	1.334 (1.313)	0.692 (0.629)	−0.398	−0.398	——
	$5/2^+$	0.678 (0.680)	−0.384 (−0.553)	−1.078	−1.078	——

C isotopes are $0.093\mu_N$ ($0.147\mu_N$) and $0.125\mu_N$ ($0.121\mu_N$) for the WBP (MK) interaction with and without the inclusion of $\delta g_\ell^{\rm IV}$, respectively. When the OFU* Hamiltonian is used, the difference of the calculated magnetic moments from those of the MK Hamiltonian amounts to be $\delta\mu=-0.01$ to $0.01\ \mu_N$, -0.07 to $-0.01\ \mu_N$, and -0.08 to $0.04\ \mu_N$ for ^{15}C, ^{17}C, and ^{19}C, respectively, which is rather minor as the rms deviation changes from $0.055\mu_N$ (MK) to $0.058\mu_N$ (OFU*) for these neutron-rich isotopes.

For ^{23}Ne ($5/2_1^+$), the two shell model interactions, WBP and MK, give rather different results since, as was stated in Sec. III A, the second $5/2_2^+$ state at $E_x=0.249$ MeV for the MK case corresponds to the ground $5/2_1^+$ state of the WBP case. The calculated magnetic moment for the WBP case is consistent with the experimental data, which supports that the Q moment should be positive, which is consistent with the HF result. The difference of the sign of the calculated magnetic moment of the $5/2_1^+$ state of ^{25}Ne between the two shell model interactions also originates from the same reason.

The rms deviations of the calculated values from the observed ones for the Ne isotopes are $0.078\mu_N$ ($0.15\mu_N$) and $0.085\mu_N$ ($0.16\mu_N$) for the WBP (MK) case with and without the effects of $\delta g_\ell^{\rm IV}$, respectively. Here, the experimental value for ^{25}Ne ($5/2^+$) is taken to be the average of the two observed data, and ^{23}Ne ($5/2^+$) is excluded from the account for the MK case because of the reason mentioned above.

The two HF interactions give always similar results in the sign and also in the magnitude of the magnetic moments. In general, the two models, the shell model and the HF model, give close results each other in most of the cases listed in Table IV and give good account of experimental data, especially in case of the shell model. Substantial differences are found only in a few cases, $3/2^-$ state in ^9C and $5/2^+$ states in ^{15}C, ^{19}Ne, and ^{21}Ne.

The calculated g factors defined by $g=\mu/J$ are shown in Fig. 6(b) for C isotopes together with experimental data. In ^{17}C, there has been controversial argument on the spin parity of the ground state. The calculated magnetic g factors are essentially the same for the two configurations $3/2^+$ and $5/2^+$ both in the shell model and the deformed HF model. These calculated g factors of the two states are both close to the experimental value. The calculated Q moments, however, are very different in the two configurations in magnitude and even in sign, reflecting the different deformation of the two configurations. The neutron and the proton contributions for the Q moment by the shell model with WBP are 17.4 mb and 6.5 mb, respectively, in the $3/2^+$ state, while they are -5.0 mb and -3.8 mb, respectively, in the $5/2^+$ state. It should be noticed that the magnetic moment and Q moment

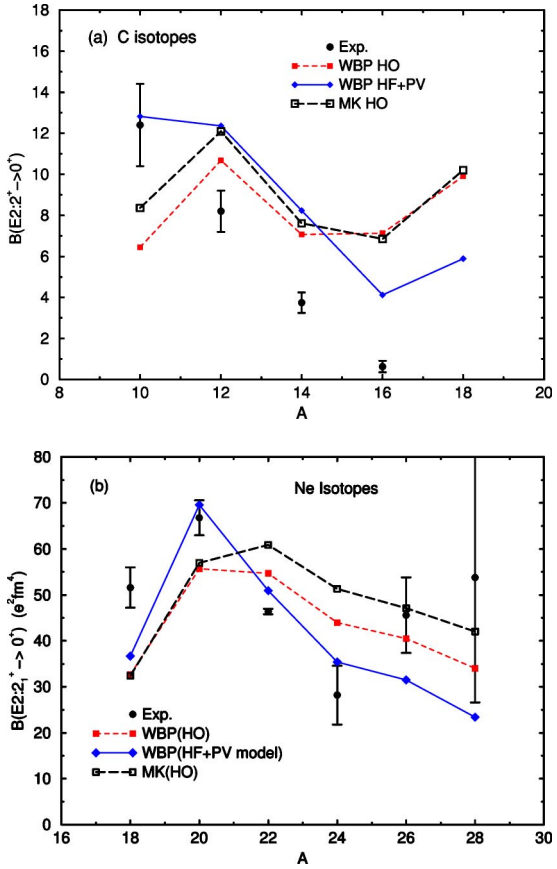

FIG. 8. (Color online) $B(E2)$ values of the $2_1^+ \rightarrow 0_{g.s.}$ transitions for (a) C isotopes and (b) Ne isotopes. Filled and open squares show the results of the shell model calculation with the use of the constant effective charges $e_p^{eff}=1.3$, $e_n^{eff}=0.5$ and the harmonic oscillator wave functions with $b=1.64$ fm for C isotopes and $b=1.83$ fm for Ne isotopes. The WBP and MK interactions are used to calculate the shell model wave functions for the filled and open squares, respectively. Filled (WBP) and open (MK) diamonds are obtained with the use of HF wave functions and the isotope dependent polarization charges e_{pol}(PV) given by Eq. (2). Filled circles show experimental values [4,30,31].

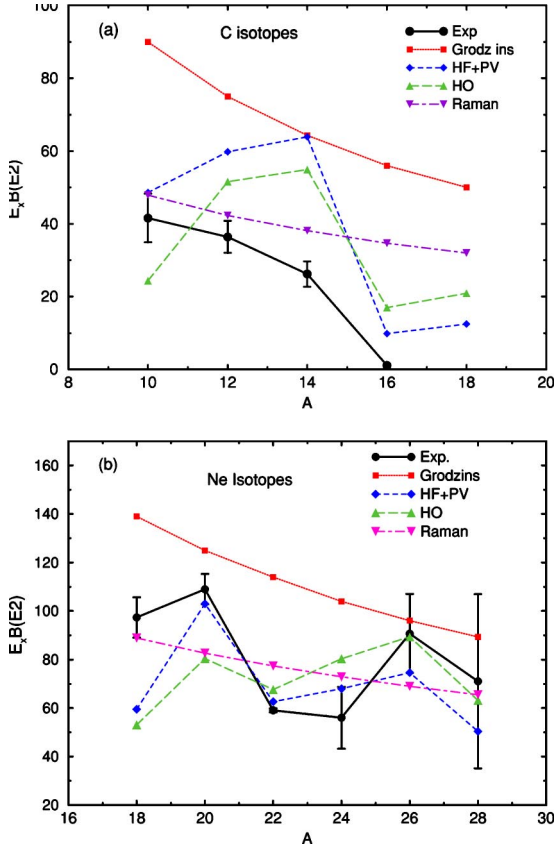

FIG. 9. (Color online) Energy weighted $B(E2)$ values of the $2_1^+ \rightarrow 0_{g.s.}$ transitions for (a) C isotopes and (b) Ne isotopes. The formulas of Grodzins and Raman systematics are given in Eqs. (14) and (15), respectively. See caption to Fig. 8 for details.

of the $3/2^+$ state in ^{17}C show large deviations from the single-particle (s.p.) values, g (Schmidt) and, Q(s.p.)$=-37.7e_{eff}(n)$ mb for the pure $0d_{3/2}$ state, i.e., even the signs of the moments between the two calculations are different. The single-particle Q moment for the pure $0d_{5/2}^+$ state is Q(s.p.)$=-53.9e_{eff}(n)$ mb, which is much larger than the shell model prediction $Q=-8.9$ mb (Notice the standard value for $e_{eff}(n)=0.5$ and the presently adopted value for ^{17}C is $e_{eff}(n)=0.33$) with the interaction WBP. It is interesting to mention that the shell model Q moments suggest the prolate deformation for the $3/2^+$ state and the oblate deformation for the $5/2^+$ state, which are consistent with the deformed HF results in Table I. The measurement of the Q moment will be the most decisive experiment to assign the spin and the parity of the ground state of ^{17}C and will provide experimental justification of the shell model and the deformed HF predictions.

The magnetic moments and the Q moment of ^{19}C are given in Tables IV and III. It is still under dispute whether the spin and the parity of the ground state of ^{19}C is $1/2^+$ or $5/2^+$ [20]. According to the shell model and the deformed HF calculations, the lowest $3/2^+$ state is also close to the lowest $1/2^+$ and $5/2^+$ states in energy. The neutron and the proton contributions to the Q moments are -15.9 mb and -14.0 mb in the $3/2^+$ state, while they are 16.3 mb for neutrons and 14.9 mb for protons in the $5/2^+$ state of ^{19}C. Notice that the proton and neutron contributions are very different from the single-particle value of the pure $0d_{5/2}^+$ state. These results suggest the large configuration mixing in the lowest $5/2^+$ state of ^{19}C. Since the magnetic moment and Q moment are very different for the three configurations in ^{19}C, measurements of these moments will give decisive information on the spin assignment of the ground state of ^{19}C.

For ^{25}Ne, the spin and the parity of the ground state are either $1/2^+$ or $3/2^+$ [29] and are not determined yet. As the magnetic moment for $1/2^+$ and $3/2^+$ are quite different, the measurement of the magnetic moment as well as the Q moment is useful for the spin assignment of the ground state of ^{25}Ne.

IV. $E2$ TRANSITIONS IN C AND Ne ISOTOPES

We discuss in this section the excitation energies and $E2$ transitions of the first 2_1^+ states in the even C and Ne iso-

TABLE V. Transition strength $B(E2)$ from the 2_1^+ states to the ground states in C isotopes. Shell model calculations are performed in a $0\,\hbar\omega$ model space in (*psd*) shell configuration with the Millener-Kurath (MK) interaction. The harmonic oscillator parameter is taken to be $b=1.64$ fm to calculate the transition matrix in the HO model. The HF wave functions for the HF+PV model are obtained by the using a Skyrme SIII interaction. The $B(E2)$ value of the shell model is calculated by using Eq. (13), while that with the deformed HF wave function is calculated from Eq. (16). Experimental $B(E2)$ values are taken from Refs. [4,30].

		Shell model		Deformed HF	
		(HO)	(HF+PV)	SGII	Expt.
^{10}C	M_n (fm^2)	−4.28	−4.43		
	M_p (fm^2)	−3.33	−3.58		
	$B(E2)$ (e^2 fm^4)	8.36	13.0	3.81	12.4±2.0
^{12}C	M_n (fm^2)	−4.31	−4.70		
	M_p (fm^2)	−4.31	−4.70		
	$B(E2)$ (e^2 fm^4)	12.1	14.7	4.86	8.2±1.0
^{14}C	M_n (fm2)	0.167	0.207		
	M_p (fm^2)	4.68	5.12		
	$B(E2)$ (e^2 fm^4)	7.61	7.99	0.0	3.74±0.50
^{16}C	M_n (fm^2)	8.20	9.82		
	M_p (fm^2)	1.35	1.72		
	$B(E2)$ (e^2 fm^4)	6.85	4.91	3.80	0.63±0.27
^{18}C	M_n (fm^2)	9.85	12.02		
	M_p (fm^2)	1.71	1.86		
	$B(E2)$ (e^2 fm^4)	10.2	5.63	5.22	——
^{20}C	M_n (fm^2)	10.32	15.74		
	M_p (fm^2)	2.97	3.38		
	$B(E2)$ (e^2 fm^4)	16.3	10.1	8.25	——

topes. The excitation energies of the first 2^+ excited states are given in Fig. 7(a) for C isotopes and in Fig. 7(b) for Ne isotopes. The shell model calculations are performed by using two effective interactions WBP and MK. The calculations with WBP and MK give good account of the observed excitation energies quantitatively in both C and Ne isotopes. The higher energy of 2_1^+ state in ^{14}C is due to the shell closure effect at $N=8$. In general, the WBP interaction predicts slightly higher excitation energies than the experimental ones, while the MK interaction gives somewhat lower excitation energies.

Calculated and experimental $B(E2)$ values for the $2_1^+ \rightarrow 0_{\mathrm{g.s}}^+$ transitions are shown in Fig. 8(a) for C isotopes and in Fig. 8(b) for Ne isotopes. The proton and neutron transition matrix elements are tabulated in Table V for C isotopes and in Table VI for Ne isotopes. We adopt two models with different kinds of effective charges and single-particle wave functions to calculate the transition strength. The first one is the constant effective charges $e_p=1.3e$ and $e_n=0.5e$ with HO wave functions. The second one is the isospin-dependent effective charges (3) with HF wave functions. The transition strength $B(E2)$ is calculated by using a formula

$$B(E2{:}I_i \rightarrow I_f) = \frac{1}{2I_i+1}|e_{eff}^n M_n + e_{eff}^p M_p|^2. \qquad (13)$$

In a proton rich-nucleus ^{10}C, Eq. (3) gives $e_{eff}^p(\mathrm{PV})=1.38$ and $e_{eff}^n(\mathrm{PV})=0.71$, which are substantially larger than the standard values. Additionally, the proton *p*-shell wave functions are extended because of a shallower proton mean field potential than that of neutrons. Combining the two effects, the $B(E2)$ value by HF+PV model is enhanced by about 50% compared with that of HO+constant effective charges and shows a good account of the experimental value. A similar enhancement of the effective charges is also pointed out in the experimental result of Q moment of ^{8}B [13]. The standard shell model and the present HF+PV model give almost the same results in nuclei ^{12}C and ^{14}C. On the other hand, in neutron-rich nuclei ^{16}C and ^{18}C, the HF+PV model gives much smaller $B(E2)$ values than those of the standard HO calculations because of the quenching of effective charges (3). The experimental data of C isotopes are decreasing constantly as a function of mass number A. This trend is qualitatively reproduced by the HF+PV model, although the calculated values are about 4 e^2 fm^4 larger than the observed ones in nuclei $^{12-16}$C. In particular, the observed $B(E2)$ value is quite smaller in ^{16}C [4] than theoretical predictions. Recently, the ^{208}Pb+^{16}C inelastic scattering was performed to determine the ratio of neutron to proton matrix element of the transition from the ground state to 2_1^+ state [5]. The observed value $(M_n/M_p)/(N/Z)=4.6\pm1.0$ can be compared with the calculated value $(M_n/M_p)/(N/Z)=3.42(3.62)$ by the HF (HO) wave functions. Both experimental and theoretical values show an unusually large contribution from neutron excitations for the 2_1^+ state in ^{16}C compared to the ratio N/Z. In Ref. [33], it was pointed out that a proton transition matrix

TABLE VI. Transition strength from the 2_1^+ states to the ground states in Ne isotopes. The harmonic oscillator parameter is taken to be $b=1.83$ fm to calculate the transition matrix in the HO model. Experimental $B(E2)$ values are taken from Ref. [30]. See the captions of Table V for details.

		Shell model		Deformed HF	
		(HO)	(HF+PV)	SGII	Expt.
^{18}Ne	M_n (fm^2)	0.0	0.0		
	M_p (fm^2)	9.79	10.04		
	$B(E2)$ (e^2 fm^4)	32.4	36.3	0.02	51.6±4.4
^{20}Ne	M_n (fm^2)	−9.38	−10.49		
	M_p (fm^2)	−9.38	−10.49		
	$B(E2)$ (e^2 fm^4)	57.0	73.0	35.9	66.8±3.8
^{22}Ne	M_n (fm^2)	−11.45	−11.59		
	M_p (fm^2)	−9.02	−9.17		
	$B(E2)$ (e^2 fm^4)	60.9	56.4	37.0	46.4±0.6
^{24}Ne	M_n (fm^2)	11.41	12.06		
	M_p (fm^2)	7.93	8.19		
	$B(E2)$ (e^2 fm^4)	51.3	43.4	9.20	28.2±6.4
^{26}Ne	M_n (fm^2)	−5.66	−6.63		
	M_p (fm^2)	−9.62	−10.0		
	$B(E2)$ (e^2 fm^4)	47.1	39.3	6.60	45.6±8.2
^{28}Ne	M_n (fm^2)	−5.18	−6.14		
	M_p (fm^2)	−9.16	−9.66		
	$B(E2)$ (e^2 fm^4)	42.0	33.5	11.4	53.8±27.2

element is strongly suppressed compared to the neutron one by a shell model calculation. The AMD model [22] predicts also a large ratio M_n/M_p, but quantitatively fails to reproduce the abnormally quenched $B(E2)$ value in ^{16}C. A consistent understanding of the two experimental data in ^{16}C is still an interesting open question. It would be also interesting to find out experimentally whether the $B(E2)$ value increases for ^{18}C, as the calculation predicts since this increase comes from a larger neutron contribution than that in ^{18}C.

The calculated $B(E2)$ values of Ne isotopes are compared with experimental data in Fig. 8(b) and Table VI. In Ne isotopes, we can see again that the enhanced $B(E2)$ value in a proton-rich nucleus ^{18}Ne and the quenched $B(E2)$ values in neutron-rich nuclei $^{22-28}$Ne in the HF+PV model compared with the standard HO model. The values calculated in HF +PV model reproduce the experimental ones better than those with HO wave functions with the constant effective charges.

In Figs. 9(a) and 9(b), the observed energy weighted transition strength $E_xB(E2)$ is compared with the present shell model results and the empirical systematics, Grodzins formula [32],

$$E_xB(E2) = (25 \pm 8)\frac{Z^2}{A} \tag{14}$$

and the formula based on the liquid drop model,

$$E_xB(E2) = 6.53\frac{Z^2}{A^{0.69}} \tag{15}$$

in Ref. [30]. It is interesting to see in C isotopes that the two shell model results with the HF+PV model and HO model show a peak at ^{14}C due to the neutron shell effect at $N=8$, while the empirical data and the systematics formulas show a monotonic decrease of the product $E_xB(E2)$. In Ne isotopes, the calculated values with HF+PV model show a peak at ^{20}Ne which is consistent with the empirical results. On the other hand, the formulas (14) and (15) show a slow smooth decrease as a function of mass A.

$B(E2)$ in the laboratory system can be expressed as

$$B(E2;KI_i \rightarrow KI_f) = \frac{5}{16\pi}(eQ_{0p})^2\langle I_iK20|I_fK\rangle \tag{16}$$

with the intrinsic Q_{0p} moment of deformed HF results. The $B(E2;K=0,I_i=2\rightarrow K=0,I_f=0)$ values are tabulated in Table V for C isotopes and in Table VI for Ne isotopes. In general, the deformed HF wave functions give smaller $B(E2)$ values compared with those of shell model calculations, especially, in the neutron closed shell nuclei ^{14}C and ^{18}Ne. On the other hand, for the well-deformed nuclei ^{20}Ne and ^{22}Ne, the HF results are comparable with both the shell model and experimental data.

Finally, we comment that considerable enhancements of the $B(E2)$ values as well as reductions of the energies of the 2_1^+ states compared to the *sd*-shell model calculations were found for very neutron-rich isotopes, $^{28-34}$Ne, by the Monte

Carlo shell model method with a modified USD-KB-MK Hamiltonian within the sd-$0f_{7/2}1p_{3/2}$ configuration space [34].

V. SUMMARY

We pointed out the strong isotope dependence of deformation of C and Ne isotopes as a clear manifestation of deformation-driving mechanism in atomic nuclei, the so-called nuclear Jahn-Teller effect by using the deformed HF calculations. The effect in light nuclei is unique compared with that in rare-earth nuclei in the sense that the prolate and the oblate deformations appear clearly in the ground states of the two isotopes. We have studied the isotope dependence of Q moments and $B(E2)$ values of C and Ne isotopes using the deformed HF wave functions and also the shell model wave functions with polarization charges obtained by the HF +PV coupling model. It is shown that the HF model is equally successful to describe observed Q moments and magnetic moments of the two isotopes as the shell model with the effective operators. The configuration dependence of the Q moments in the odd C isotopes, which can be attributed to the shell effects, is pointed out by using both the HF and the shell model wave functions. This dependence can be used to determine unknown spin parities as well as the deformation properties of the ground states of neutron-rich C and Ne isotopes. The isotope dependence of the $B(E2)$ values in even C and Ne isotopes are reproduced well by the shell model calculations with the isospin-dependent polarization charges, while the standard shell model calculations with HO wave functions and the constant effective charges fail to reproduce the isotope dependence of $B(E2)$ values. There is still an open question whether the extremely quenched experimental $B(E2)$ value in ^{16}C is attributed to further quenching of neutron polarization charge or exotic shapes of proton and neutron density distributions.

ACKNOWLEDGMENTS

We thank K. Hagino, W. Nazarewicz, T. Nakatsukasa, and M. Kawai for stimulating and enlightening discussions. This work is supported in part by the Japanese Ministry of Education, Culture, Sports, Science and Technology by a Grant-in-Aid for Scientific Research under Program No. (C (2)) 16540259.

[1] I. Tanihata *et al.*, Phys. Rev. Lett. **55**, 2676 (1985); P. G. Hansen and B. Jonson, Europhys. Lett. **4**, 409 (1987); I. Tanihata, J. Phys. G **22**, 157 (1996).
[2] A. Ozawa, T. Kobayashi, T. Suzuki, K. Yoshida, and I. Tanihata, Phys. Rev. Lett. **84**, 5493 (2000).
[3] A. Leistenschneider, T. Aumann, K. Boretzky, D. Cortina, J. Cub, U. Datta Pramanik, W. Dostal, Th. W. Elze, H. Emling, H. Geissel, A. Grünschloß, M. Hellstr, R. Holzmann, S. Ilievski, N. Iwasa, M. Kaspar, A. Kleinbh, J. V. Kratz, R. Kulessa, Y. Leifels, E. Lubkiewicz, G. Münzenberg, P. Reiter, M. Rejmund, C. Scheidenberger, C. Schlegel, H. Simon, J. Stroth, K. Sümmerer, E. Wajda, W. Walús, and S. Wan, Phys. Rev. Lett. **86**, 5442 (2001).
[4] N. Imai *et al.*, Phys. Rev. Lett. **92**, 062501 (2004).
[5] Z. Elekes *et al.*, Phys. Lett. B **586**, 34 (2004).
[6] H. A. Jahn and E. Teller, Proc. R. Soc. London, Ser. A **161**, 220 (1937).
[7] P.-G. Reinhard and E. W. Otten, Nucl. Phys. **A420**, 173 (1984).
[8] W. Nazarewicz, Int. J. Mod. Phys. E **2**, 51 (1993); Nucl. Phys. **A574**, 27c (1994).
[9] B. A. Brown, Prog. Part. Nucl. Phys. **45**, 517 (2001).
[10] A. Bohr and B. R. Mottelson, *Nuclear Structure*, Vol. 2 (Benjamin, Massachusetts, 1975).
[11] H. Sagawa and K. Asahi, Phys. Rev. C **63**, 064310 (2001).
[12] H. Sagawa, Phys. Rev. C **65**, 064314 (2002).
[13] T. Minamizono *et al.*, Phys. Rev. Lett. **69**, 2058 (1993); H. Izumi *et al.*, Phys. Lett. B **366**, 51 (1996); H. Ogawa *et al.*, Phys. Rev. C **67**, 064308 (2003).
[14] D. J. Millener and D. Kurath, Nucl. Phys. **A255**, 315 (1975).
[15] E. K. Warburton and B. A. Brown, Phys. Rev. C **46**, 923 (1992); OXBASH, the Oxford, Buenos-Aires, Michigan State, Shell Model Program, B. A. Brown *et al.*, MSU Cyclotron Laboratory Report No. 524 (1986).
[16] T. Suzuki, H. Sagawa, and K. Hagino, Phys. Rev. C **68**, 014317 (2003).
[17] T. Suzuki, H. Sagawa, and K. Hagino, in the *Proceedings of the International Symposium on Frontiers of Collective Motions (CM2002)* (World Scientific, Singapore, 2003), p. 236; H. Sagawa, T. Suzuki, and K. Hagino, Nucl. Phys. **A722**, 183 (2003).
[18] M. Bender, K. Rutz, P.-G. Reinhard, and J.A. Maruhn, Eur. Phys. J. A **8**, 59 (2000).
[19] H. Ogawa, K. Asahi, H. Ueno, K. Sakai, H. Miyoshi, D. Kameda, T. Suzuki, H. Izumi, N. Imai, Y.X. Watanabe, K. Yoneda, N. Fukuda, H. Watanabe, A. Yoshimi, W. Sato, N. Aoi, M. Nagakura, T. Suga, K. Yogo, A. Goto, T. Honda, Y. Kobayashi, W.-D. Schmidt-Ott, G. Neyens, S. Teughels, A. Yoshida, T. Kubo, and M. Ishihara, Eur. Phys. J. A **13**, 81 (2002).
[20] D. Bazin *et al.*, Phys. Rev. C **57**, 2156 (1998); T. Nakamura *et al.*, Phys. Rev. Lett. **83**, 1112 (1999); V. Maddalena *et al.*, Phys. Rev. C **63**, 024613 (2001).
[21] Rituparna Kanungo, I. Tanihata, Y. Ogawa, H. Toki, and A. Ozawa, Nucl. Phys. **A677**, 171 (2000).
[22] Y. Kanada-En'yo and H. Horiuchi, Prog. Theor. Phys. **142**, 205 (2001). Y. Kanada-En'yo (private communications).
[23] T. Suzuki, R. Fujimoto, and T. Otsuka, Phys. Rev. C **67**, 044302 (2003); T. Otsuka, R. Fujimoto, Y. Utsuno, B. A. Brown, M. Honma, and T. Mizusaki, Phys. Rev. Lett. **87**, 082502 (2001).
[24] P. Raghaven, At. Data Nucl. Data Tables **42**, 189 (1989).
[25] K. Matsuta *et al.*, Nucl. Phys. **A588**, 153c (1995).
[26] T. Suzuki, in *Proceedings of the International Conference*

Structure of the Nucleus at the Dawn of the Century, Bologna, 2000, edited by G. C. Bonsignori, M. Bruno, A. Ventura, and D. Vretenar (World Scientific, Singapore, 2001).

[27] K. Asahi, K. Sakai, H. Ogawa, H. Ueno, Y. Kobayashi, A. Yoshimi, H. Miyoshi, K. Yogo, A. Goto, T. Suga, N. Imai, Y.X. Watanabe, K. Yoneda, N. Fukuda, N. Aoi, W.-D. Schmidt-Ott, G. Neyens, S. Teughels, A. Yoshida, T. Kubo, and M. Ishihara, AIP Conf. Proc. 570, 109 (2001).

[28] A. Arima and H. Hyuga, in *Mesons in Nuclei*, edited by M. Rho and D. Wilkinson (North-Holland, Amsterdam, 1979), Vol. II, p. 683; T. Yamazaki, in *Mesons in Nuclei*, Vol. II, edited by M. Rho and D. Wilkinson (North-Holland, Amsterdam, 1979), p. 651.

[29] *Table of Isotopes*, edited by R. B. Firestone *et al.* (Wiley, New York, 1996).

[30] S. Raman *et al.*, At. Data Nucl. Data Tables **36**, 1 (1987).

[31] B. V. Pritychenko *et al.*, Phys. Lett. B **461**, 322 (1999).

[32] L. Grodzins, Annu. Rev. Nucl. Sci. **18**, 291 (1968).

[33] R. Fujimoto, Ph.D. thesis, University of Tokyo (2003).

[34] Y. Utsuno, T. Otsuka, T. Mizusaki, and M. Honma, Phys. Rev. C **60**, 054315 (1999).